CALCIUM CURRENTS IN RAT THALAMOCORTICAL RELAY NEURONES: KINETIC PROPERTIES OF THE TRANSIENT, LOW-THRESHOLD CURRENT

By DOUGLAS A. COULTER, JOHN R. HUGUENARD*
AND DAVID A. PRINCE

From the Department of Neurology, Stanford University Medical Center, Stanford, CA 94305, USA

SUMMARY

1. Calcium currents were recorded with whole-cell voltage-clamp procedures in relay neurones of the rat thalamus which had been acutely isolated by an enzymatic dissociation procedure.

2. Low-threshold and high-threshold Ca^{2+} currents were elicited by depolarizing voltage steps from holding potentials more negative than -60 mV. A transient current, analogous to the T-current in sensory neurones, was activated at low threshold near -65 mV and was completely inactivating at command steps up to -35 mV. Voltage steps to more depolarized levels activated a high-threshold current that inactivated slowly and incompletely during a 200 ms step depolarization.

3. The high-threshold current contained both non-inactivating and slowly inactivating components which were insensitive and sensitive to holding potential, respectively.

4. A 'T-type' current was prominent in relay neurones, in both absolute terms (350 pA peak current average) and in relation to high-threshold currents. The average ratio of maximum transient to maximum sustained current was greater than 2.

5. T-current could be modelled in a manner analogous to that employed for the fast Na^+ current underlying action potential generation, using the m^3h format. The rate of activation of T-current was voltage dependent, with a time constant (τ_m) varying between 8 and 2 ms at command potentials of -60 to -10 mV at 23 °C. The rate of inactivation was also voltage dependent, and the time constant τ_h varied between 50 and 20 ms over the same voltage range. With command potentials more positive than -35 mV, the inactivation of Ca^{2+} current could no longer be fitted by a single exponential.

6. Steady-state inactivation of T-current could be well fitted by a Boltzman equation with slope factor of 6·3 and half-inactivated voltage of $-83\cdot5$ mV.

7. Recovery from inactivation of T-current was not exponential. The major component of recovery (70–80 % of total) was not very voltage sensitive at potentials more negative than -90 mV, with τ_r of 251 ms at -92 mV and 23 °C, compared to

* To whom all correspondence and reprint requests should be addressed.

225 ms at -112 mV. A smaller, voltage-sensitive component accounted for the remainder of recovery.

8. All kinetic properties, including rates of activation, inactivation, and recovery from inactivation, as well as the amplitude of T-current, were temperature sensitive with Q_{10} (temperature coefficient) values of greater than 2·5.

9. These properties of the T-current are such that its activation is necessary and sufficient to cause the generation of low-threshold calcium spikes in thalamic relay neurones, although other ionic conductances may modulate such events.

INTRODUCTION

A prominent burst-firing response is one of the characteristic properties of thalamic relay neurones, as revealed by *in vivo* intracellular recordings in cat (Deschênes, Roy & Steriade, 1982; Deschênes, Paradis, Roy & Steriade, 1984) as well as *in vitro* studies in thalamic slices of guinea-pig (Jahnsen & Llinás, 1984*a, b*) and rat (Crunelli, Kelly, Leresche & Pirchio, 1987). The burst is characterized by a low-threshold spike (LTS) which can be evoked either by depolarizing current injection or orthodromic synaptic excitation when the resting membrane potential is more negative than approximately -60 mV. The LTS is a Ca^{2+}-dependent, slow (20–50 ms), 10–30 mV envelope of depolarization that can in turn trigger multiple Na^+-dependent action potentials.

Although the Ca^{2+}-dependent LTS plays a significant role in determining the spike firing pattern of neurones in a number of brain areas including thalamus (Jahnsen & Llinás, 1984*b*), inferior olive (Llinás & Yarom, 1981), pontine reticular formation (Greene, Haas & McCarley, 1986), habenula (Wilcox, Gutnick & Christoph, 1988), and some neocortical areas (Friedman & Gutnick, 1987), the characteristics of the underlying transient Ca^{2+} current have not been examined. The LTS burst-firing mechanism is particularly important in determining the response characteristics of thalamocortical relay neurones (Deschênes, *et al.* 1984; Jahnsen & Llinás, 1984*a*). Rhythmic burst firing in these cells is correlated with behavioural states such as slow-wave sleep (reviewed in Steriade & Llinás, 1988) and may be important in generating pathological thalamocortical rhythms such as spike-wave discharges in petit mal epilepsy (Coulter, Huguenard & Prince, 1989).

There are a number of ionic conductances present in relay neurones (Jahnsen & Llinás, 1984*b*) that may contribute to the generation of the LTS, including (1) a low-threshold Ca^{2+} current activated by depolarization from hyperpolarized potentials, (2) a persistent, tetrodotoxin-sensitive, low-threshold Na^+ conductance activated by depolarization, and (3) an anomalous rectifier current activated by hyper-polarization. However, the Ca^{2+}-dependent component appears to be the major factor in generating the LTS, since removal of extracellular Ca^{2+} or the addition of Ca^{2+} channel blockers such as Cd^{2+} abolish the LTS, while the latter is unaffected by tetrodotoxin which blocks Na^+ currents (Jahnsen & Llinás, 1984*b*). Several types of neuronal Ca^{2+} currents have been identified in sensory neurones of the rat and chick dorsal root ganglion (Carbone & Lux, 1984; Nowycky, Fox & Tsien, 1985) and the activation properties of one of these, the low-threshold or 'T' current, are such that it may be implicated in the generation of the LTS. We have undertaken a voltage-

clamp study to characterize the Ca^{2+} currents in thalamic relay neurones acutely isolated from non-embryonic tissue (Kay & Wong, 1986). The somatosensory ventrobasal complex (VB) of the rat was chosen as the source of thalamic neurones because in rodents this set of nuclei contains a nearly pure population of relay cells; there are less than 1 % interneurones (Jones, 1985; Harris & Hendrickson, 1987). The major focus of this report is on the voltage-dependent properties of the low-threshold transient (T-type) current in these cells.

METHODS

Preparation and enzymatic isolation procedure

Since interneurones might be selectively spared during the trauma of the dissociation procedure described below, we initially used an antibody to glutamic acid decarboxylase (GAD), kindly provided by Dr Donald Schmechel, and standard immunocytochemical techniques to assess the numbers of GABA(γ-aminobutyric acid)ergic neurones in our dissociated neuronal preparation. Only rare cells obtained from VB in isolation reacted positively for the presence of GAD (not shown), and these were easily distinguished from the larger relay neurones.

All experiments were carried out using cells isolated from 2- to 25-day-old Wistar rats. Dissociation methods were modified from those of Kay & Wong (1986). Pregnant rats were obtained at 18 days gestation from Simonsen Laboratories (Gilroy, CA, USA) and were housed in our animal facility. Rat pups were anaesthetized with pentobarbitone, decapitated, and the brains removed and placed in cold saline (4 °C) for 1–2 min. The brain was then blocked and sectioned in the coronal plane using a Lancer vibratome (St Louis, MO, USA). Slices (500 μm) that contained the ventrobasal (VB) complex were dissected by scalpel cuts to isolate the thalamus. VB was identified as a crescent-shaped area, demarcated on its lateral and ventral borders by the external medullary lamina, medial lemniscus and reticular nucleus. In the youngest animals, where myelination was less complete, VB was identified by comparing living slices with an atlas made from Nissl stains of comparably aged animals. Thalamic slices were then incubated for 45–90 min in an oxygenated PIPES-buffered saline (see Solutions) containing trypsin (Type XI, 8 mg/10 ml). After enzymatic treatment, the slices were washed in trypsin-free PIPES saline, and VB was isolated with scalpel cuts. Once isolated, each VB section was divided in half, triturated with fire-polished Pasteur pipettes, and plated onto 35 mm plastic Petri dishes (Lux tissue culture dishes, Miles Scientific, Naperville, IL, USA). Isolated relay neurones were somewhat variable in appearance but a majority had relatively large somata (15–25 μm), and several thick (2–3 μm) dendrites extending for up to 80 μm from the soma. These neurones survived for up to 12 h following isolation.

Solutions

A PIPES-buffered saline was used in all steps prior to recording currents. It consisted of (in mM): NaCl, 120; KCl, 5; $MgCl_2$, 1; $CaCl_2$, 1; glucose, 25; piperazine-N,N'-bis(2-ethanesulphonic acid) (PIPES), 20; and the pH was adjusted to 7·0 with NaOH (Kay & Wong, 1986). For whole-cell recording of Ca^{2+} currents the following solutions were used. Intracellular solution (mM): Tris-PO_4 (dibasic), 110; Tris base, 28; EGTA, 11; $MgCl_2$, 2; $CaCl_2$, 0·5; Na_2 ATP, 4; pH 7·3. Extracellular solution (mM): NaCl, 155; KCl, 3; $MgCl_2$, 1; $CaCl_2$, 3; tetrodotoxin, 0·0005; HEPES, 10; and pH adjusted to 7·4 with NaOH. All chemicals were obtained from Sigma (St Louis, MO, USA).

Electrophysiological recordings

Isolated relay neurones were voltage clamped using the whole-cell configuration of the patch clamp (Hamill, Marty, Neher, Sakmann & Sigworth, 1981). Electrodes were pulled from thick-walled borosilicate glass (H15/10/181, Jencons Ltd, Leighton Buzzard) on a List L/M-3P-A (Medical Systems, Great Neck, NY, USA) puller using a two-step procedure. When filled with intracellular Tris-PO_4 solution, electrode resistances were 5–8 MΩ. An 8 mV liquid junction potential was measured between the intracellular and extracellular solutions (see Hagiwara & Ohmori, 1982), and this correction was applied *post facto* to all command potentials. Current recordings were obtained with either the List EPC-7 (Medical Systems) or the Axopatch 1A

amplifier (Axon Instruments, Burlingame, CA, USA). In either case, series resistance compensation was used to eliminate 90% of the voltage error due to the passage of current through the patch pipette. Access resistance was normally in the range of 6–10 MΩ. Inward Ca^{2+} currents were always less than 1 nA with a resulting maximum series resistance error smaller than 1 mV, when compensated by 90%.

A modified subtraction technique (based on Bezanilla & Armstrong, 1977) was used to remove interference from linear leak and capacitative currents. Several scaled hyperpolarizing leak pulses were applied from a reduced holding potential (-50 mV) before the holding potential was increased to conditioning potential (normally -100 mV) for 1 s preceding the command step. Stimuli were normally applied at < 0.1 Hz. These protocols allowed Ca^{2+} currents to be recorded in relay neurones for up to 75 min. Ca^{2+} current records obtained by linear leak subtraction were indistinguishable from those in experiments where the leak and capacitative currents were obtained by applying the normal stimulation protocol to a neurone bathed in normal extracellular saline with 0.5 mM-$CdCl_2$ added to block Ca^{2+} currents.

Voltage-clamp control was judged by several criteria, including (1) smooth voltage-dependent current activation, (2) lack of excessive delay in onset of current, and (3) onset and offset kinetics that were dependent on voltage but *not* on the amplitude of current (see Results). Only cells in which adequate clamp conditions were obtained using these criteria were included in this kinetic study. Isopotentiality of neuronal membrane was assured by testing the exponentiality of the capacitative transient (Kay & Wong, 1987).

Most experiments were performed at room temperature (22–24 °C) since survival of isolated cells was prolonged under these conditions. For experiments where temperature dependence was determined, the chamber which encased the Petri dishes was warmed by a feedback-controlled resistive heater. Bath temperature was monitored with a small thermocouple placed in the chamber within 100 μm of the neurone under study.

Data storage and analysis

Data were sampled on line in either unsubtracted or leak-subtracted form using a DEC 11-73 based computer equipped with the Cheshire interface (Indec Systems, Sunnyvale, CA, USA) running under BASIC-23. Currents and command voltages were also recorded in pulse code modulated form (Neurocorder, Neurodata, NY, USA) and stored on videotape for back-up purposes. For kinetic fits to current records, an iterative approach was used in which the parameters were adjusted by means of the analog inputs on the Cheshire interface. This method was found to provide a rapid means of fitting onsets and exponential decays with up to two components. A non-linear least-squares fitting routine (Schreiner, Kramer, Krischer & Langsam, 1985) was used to verify these results in representative traces; the fits obtained by these two methods were not significantly different (see Results) in the rate constants or amplitudes of the various components.

RESULTS

Ca^{2+} currents in relay neurones

Dissociated relay neurones were similar to several other types of isolated central neurones in that they were normally truncated at the level of the primary or secondary dendrites, and had very low input conductance when measured in the whole-cell clamp mode (Numann & Wong, 1984; Huguenard & Alger, 1986; Kay & Wong, 1987), normally less than 1 nS. Inward currents could often be recorded, even in unsubtracted traces. With the use of the appropriate solutions, Ca^{2+} currents were readily obtained. When depolarizing step commands were applied from a holding potential of -100 mV, Ca^{2+} current components with different onset and decay kinetics were seen at various command potentials (Fig. 1). Small depolarizations to between -60 and -40 mV resulted in a rapidly activating inward current that completely inactivated within a 200 ms depolarization. The rate of current decay became more rapid with increasing depolarizations within this voltage range. With

stronger depolarizations (more positive than -40 mV) the current was incompletely inactivating during the depolarization, and the rate of current decay became slower (e.g. compare currents at -20 through to 0 mV command steps in Fig. 1). These transient and sustained currents and the *I–V* relationships for the different components shown in Fig. 2 are similar to those seen in sensory neurones (Fox,
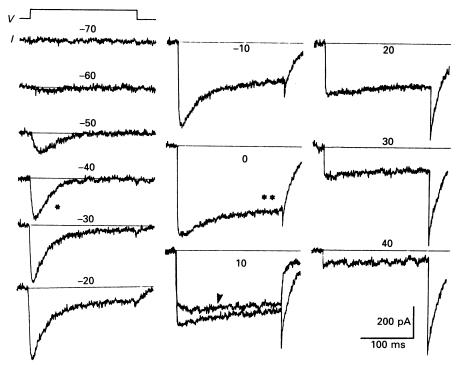

Fig. 1. Thalamic calcium currents. Leak-subtracted traces are shown for step depolarizations to the indicated command potentials (mV) from a holding potential of -100 mV. The maximum isolated transient current is obtained at -40 mV (*); with more depolarized commands a persistent component is seen, which becomes maximal near 0 mV (**). When the holding potential was reduced to -30 mV, the transient components of the current disappeared, but the persistent component remained at almost the same level. For example, the current obtained with depolarization to $+10$ mV from reduced holding potential, V_{hold}, is shown at the arrowhead (middle column). The voltage protocol (*V*) is indicated above the first column and the current traces (*I*) below.

Nowycky & Tsien, 1987; Carbone & Lux, 1987). The transient component was prominent in the low-threshold range, with an activation threshold near -60 mV and a peak near -25 mV (Fig. 2). There was also a smaller high-threshold transient component activated at commands more positive than -10 mV, which was usually less than 25 % of the amplitude of the low-threshold transient component. The low-threshold transient component appears analogous to the type I current characterized in neuroblastoma (Narahashi, Tsunoo & Yoshii, 1987) or low-voltage-activated current in sensory neurones (Carbone & Lux, 1984), which has also been termed the T-current (Nowycky *et al.* 1985; Fox *et al.* 1987). The higher threshold component of

the transient current has properties similar to the N-current of Fox *et al.* (1987), in that the rate of inactivation is relatively voltage independent, with a time constant of 90–100 ms in the voltage range of -30 to $+30$ mV. The 'N' type of inactivating current of thalamic cells was different from that in sensory neurones since it made a relatively small contribution to the total high-threshold current. The final Ca^{2+}-
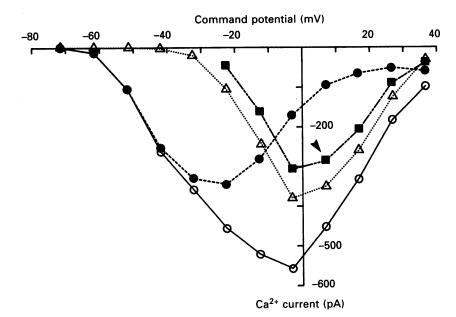

Fig. 2. Current–voltage relationship for the traces in Fig. 1. Peak ($\bigcirc$), sustained ($\triangle$, 200 ms latency), and transient ($\bullet$, difference between peak and sustained) current amplitudes are shown. In this cell, maximum transient current was 348 pA and maximum sustained current was 403 pA. The amplitude of sustained currents obtained with reduced V_{hold} (-30 mV, $\blacksquare$) is only slightly less than that obtained with the more hyperpolarized V_{hold}. The point indicated by the arrow-head is the amplitude for the corresponding trace in Fig. 1.

dependent component is the sustained, high-voltage-activated, or L-current, which was activated at a threshold near -40 mV and peaked at command potentials near 0 mV (Fig. 2, $\triangle$). As in sensory neurones (Carbone & Lux, 1984; Nowycky *et al.* 1985) and neuroblastoma (Narahashi *et al.* 1987), the L-current was relatively insensitive to steady-state inactivation; steady-state currents of similar amplitudes were obtained from holding potentials of -30 and -100 mV (Fig. 2, $\blacksquare$).

All components of inward current were clearly Ca^{2+} dependent. The maximum peak, steady-state, and transient currents were increased by 36 ± 3, 28 ± 5 and $45\pm15\%$ (mean$\pm$S.E.M., $n = 3$), respectively, when $[Ca^{2+}]_o$ was raised from 3 to 11 mM. Under these conditions, the command potentials at which maximum currents were reached were shifted in the positive direction by 7–10 mV, as expected from the increase in divalent screening charge (Frankenhaeuser & Hodgkin, 1957; Hille, 1968). Substitution of equimolar Ba^{2+} for Ca^{2+} resulted in comparable 'T' currents, while high-threshold currents were increased in amplitude and exhibited slower inactivation kinetics. In the presence of 0·5 mM-Cd^{2+} or 0·1 mM-La^{3+}, both transient

and persistent current components were blocked or reduced to 1–10 % of control levels, while 20 μM-Cd^{2+} selectively blocked high-threshold currents and 100 μM-Ni^{2+} selectively reduced 'T' current (not shown), as in sensory neurones (Fox *et al.* 1987). Inward current traces were not contaminated by concomitant activation of K^+ conductances since replacement of extracellular Na^+ and K^+ with tetraethyl-ammonium chloride did not alter the currents (not shown).

With command steps positive to -35 mV, a slow time course ($\tau_{inactivation} \approx 50$ ms, see Fig. 1) tail current was activated which was not Ca^{2+} dependent. In cells with large depolarization-activated Ca^{2+} currents which were blocked by 0·5 mM-Cd^{2+}, the tail current was either not affected or only slightly reduced. This tail current bears some resemblance to I_x seen in hippocampal neurones (Kay & Wong, 1987). Since all depolarization-activated currents were blocked by Cd^{2+} we presume that activation of the conductance underlying I_x does not interfere with the isolation of I_{Ca} at depolarized potentials.

A characteristic feature of Ca^{2+} currents recorded in relay neurones was a large low-threshold transient or 'T-type' current component, both in absolute terms and relative to the size of other components. Based on the similarities in voltage dependence, Ba^{2+} permeation and sensitivity to Ni^{2+} and Cd^{2+}, we have adopted the nomenclature of Fox *et al.* (1987) and will refer to the low-threshold transient current as T-current. The cell in Fig. 2 had over 300 pA of T-current and a ratio near 1:1 for maximum inactivating to maximum sustained current ($I:S$); in many cells this ratio was much greater than unity. After allowing 4–5 min for the intracellular perfusate to reach equilibrium, both transient and sustained components of Ca^{2+} current were relatively stable during the remaining period of recording (typically 15–30 min in this series of experiments). Therefore, the high ratio of $I:S$ was not due to differential run-down of the L-current, which was effectively maintained at a stable amplitude by the inclusion of ATP in the pipette solution. It has been suggested that high-threshold Ca^{2+} channels are localized in the dendrites (Jahnsen & Llinás, 1984b), and since the dendrites are significantly truncated by the dissociation, it could be argued that isolated cells would have a less prominent high-threshold component. However, we found no apparent correlation between the remaining dendritic area and the amplitude of the L-current in a given dissociated neurone. For example, some cells with multiple primary and some secondary dendrites had small L-currents, while others which were truncated at the level of primary dendrites had large L-currents. In a group of forty-nine cells, the maximum inactivating current (always recorded near -20 mV) was 350 ± 27 pA, the maximum sustained current was 284 ± 25 pA, with a overall average ratio ($I:S$) of 1·23:1 (Fig. 3A). The average ratio within individual relay neurones was $2·62 \pm 0·67$ (Fig. 3B). The discrepancy between these two ratios may be due to different subpopulations of relay neurones that possess varying relative sizes of inactivating (mainly T with a small contribution from N) *vs.* sustained (L) currents. Anatomical subclasses of relay neurones in VB are known (see Jones, 1985) which could, in theory, have different physiological properties, as is true in the dorsal lateral geniculate nucleus (Crunelli, Leresche & Parnavelas, 1987).

Although relay neurones possess both low- and high-threshold Ca^{2+} conductances, it is the prominent low-threshold current that underlies some of their unique physiological behaviour (Steriade & Llinás, 1988). We therefore examined the voltage-dependent kinetic properties of the T-current in some detail.
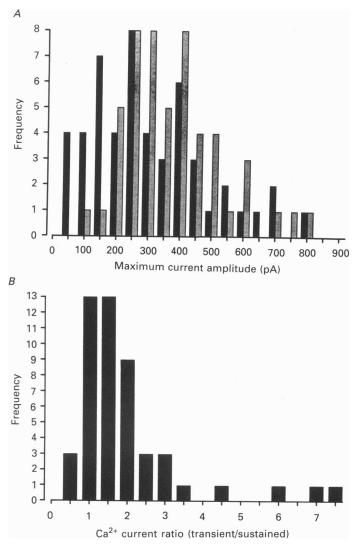
Fig. 3. Ca²⁺ current magnitudes in isolated relay neurones. *A*, histogram of peak current amplitude for forty-nine neurones. Maximum amplitudes for transient (■) and the sustained (■) currents were obtained from *I–V* curves as in Fig. 2. *B*, histogram of ratios of peak transient to peak sustained current within neurones.

Kinetics of activation and inactivation of T-current in relay neurones

Since the T-current displays a number of properties similar to those of the fast Na⁺ current underlying the action potential (Hodgkin & Huxley, 1952), we applied a similar model to the analysis of its voltage-dependent kinetics. The time course of the onset of T-current was sigmoidal in that there was a clear delay or 'foot' on the rising phase of the current. We applied different models to describe the time course of current onset, according to the following general equation:

$$I_{Ca} = [1 - \exp{(-t/\tau_m)}]^N \exp{(-t/\tau_h)} I_{\infty}, \tag{1}$$

where τ_m is the time constant of activation, N is a whole number between 1 and 4, τ_h is the time constant of inactivation, and I_∞ is the current level that would be reached in the absence of inactivation (Hodgkin & Huxley, 1952). The best fit was obtained with an $N = 3$ (m^3); m or m^2 produced too little delay and m^4 resulted in excessive delay (Fig. 4). With command potentials more negative than -35 mV, the
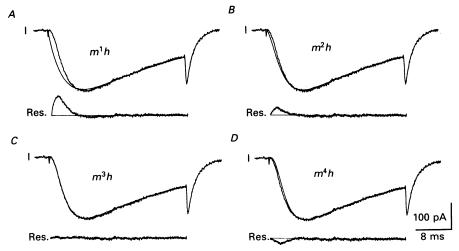

Fig. 4. Activation kinetics of T-current in relay neurone. The current trace used for the fits was obtained from the average of twenty depolarizations to -42 mV from a holding potential of -102 mV, using a P/16 subtraction procedure. A sigmoidal onset phase of the T-current is clearly apparent. Curve fits were obtained by eye for various models including m^1h, m^2h, m^3h and m^4h. The residual (Res.) difference between the data and the fitted curve is shown for each model. The m^3h model obtains the best fit for the onset rate of the T-current. The parameters were as follows: A (extrapolated initial current amplitude) $= -340$ pA and $\tau_h = 26\cdot0$ ms for all models; τ_m was $3\cdot8$, $2\cdot4$, $2\cdot1$ and $1\cdot9$ ms for m^1h–m^4h, respectively. Non-linear least-squares parameters for the m^3h fit were: $A = -337$ pA, $\tau_h = -25\cdot6$ ms and $\tau_m = -2\cdot08$ ms.

inactivation phase was well described by a single-exponential decay process. With more positive commands, however, the time course of decay became more complicated, with best fit assuming two or more components. The confidence in the fit of such complicated waveforms is necessarily lower than for simple fits, so the most reliable information on voltage-dependent kinetics is obtained in the low-threshold range where T-current is activated in isolation, i.e. more negative than -35 mV.

Both activation and inactivation of T-current were voltage dependent, becoming faster with depolarization, such that the duration and latency to peak become shorter with increasing depolarizations (Fig. 5A and B). The activation (m) phase was smoothly voltage dependent, with values for τ_m gradually varying from 8 to 2 ms in the voltage range -60 to -10 mV at 23 °C (Fig. 5C). The decay (h) phase was also voltage dependent, with values for τ_h varying between 50 and 20 ms, in the same voltage range (Fig. 5D). At potentials more positive than -40 mV, the voltage dependence appeared to decrease, although the above-mentioned inability to obtain reliable curve fits at these potentials made it difficult to quantify this effect reliably.

The activation process was smoothly voltage dependent (Fig. 6*C*) and could be described by a Boltzman equation of the following form:

$$p_{Ca} = \bar{p}_{Ca}/\{1 + \exp[(V_{\frac{1}{2}} - V)/k]\}^N, \qquad (2)$$

where $\bar{p}_{Ca}$ is the maximum permeability, $V_{\frac{1}{2}}$ is the potential at which the permeability is half-maximal, V is the command potential, k is the slope factor, and N is a power
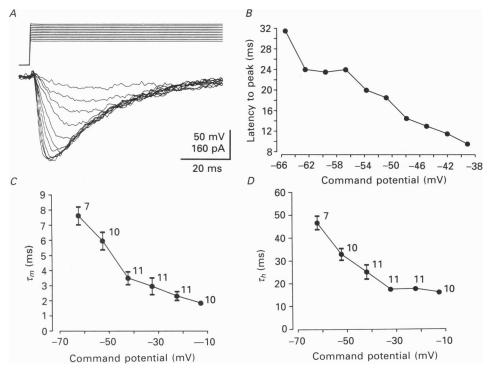

Fig. 5. Voltage-dependent kinetics of T-current. *A*, T-current responses to small (3 mV) increments in command potential in the range −60 to −33 mV. With increasing depolarization, the currents become larger with faster onset and decay. *B*, peak latencies for experiment shown in part *A*. *C*, voltage dependence of the time constant of activation (τ_m) of T-current. *D*, voltage dependence of the time constant of inactivation (τ_h) of T-current. The numbers adjacent to the data points in parts *C* and *D* are the number of neurones from which kinetic fits were made. Error bars are one S.E.M.

factor of 3. The activation function was determined by dividing the extrapolated zero-time current (from the m^3h fits) by the constant-field equation (Goldman, 1943; Hodgkin & Katz, 1949; see Kay & Wong, 1987). Threshold for activation was near −65 mV, and the current was half-maximally activated at −52 mV.

Steady-state inactivation of T-current in relay neurones

As current-clamp recordings have revealed (Jahnsen & Llinás, 1984*a*; Deschênes *et al.* 1984), the conductance underlying the low-threshold spike in relay neurones is inactivated at resting membrane potentials near −60 mV. To examine the corresponding property of the T-current in more detail, steady-state inactivation

was determined by applying 1 s conditioning pulses at various potentials followed by test pulses to -42 mV (Fig. 6A). Fractional current (normalized to the maximum current) was fitted with the following equation:

$$I/I_{max} = 1/\{1 + \exp[(V - V_{\frac{1}{2}})/k]\}. \tag{3}$$

Best fit for averaged fractional steady-state inactivation was obtained with $V_{\frac{1}{2}} = 83 \cdot 5$ and $k = 6 \cdot 3$ (Fig. 6C). At potentials more positive than -60 mV, less than 3 % of the
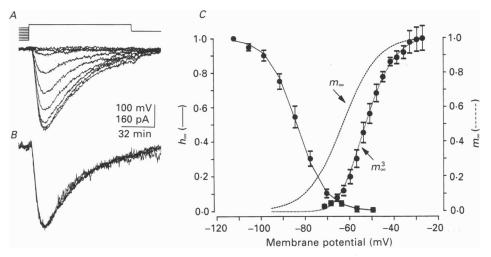

Fig. 6. Voltage dependence of steady-state inactivation and activation of T-current. A, test depolarizations to -42 mV were preceded by 1 s conditioning steps at various membrane potentials between -112 and -62 mV. B, currents obtained with holding potentials of -102, -92, -82, -72 and -62 mV are normalized to peak current amplitude. Activation and inactivation kinetics were independent of the amplitude of the current. C, average fractional inactivation (h_∞, $n = 12$) and activation (m_∞, $n = 14$). The continuous smooth curve is the best-fit Boltzman function for steady-state inactivation with $V_{\frac{1}{2}} = -83 \cdot 5$ mV and $k = 6 \cdot 3$. For activation the best fit (m_∞^3, dotted line) was obtained with $V_{\frac{1}{2}} = -63$ mV and $k = 7 \cdot 8$. Also shown is the m_∞ curve (dashed line). Initial current amplitudes were determined from m^3h fits and converted to activation by dividing by the constant-field equation. Error bars represent 1 S.E.M.

total T-current is available for activation, and hyperpolarizations beyond -100 mV are required to completely remove inactivation. The existence of multiple components which might contribute to the low-threshold Ca^{2+} current would be indicated by changes in the time course of activation or inactivation with different conditioning potentials, assuming these separate components had different kinetic properties and different steady-state inactivation. Responses obtained at a command potential of -42 mV from various holding potentials are shown in Fig. 6A. The equivalent onset and offset kinetics of the superimposed currents (Fig. 6B) provides evidence for a single current component underlying the low-threshold burst response. In isolated relay neurones, T-current kinetics at a given command potential were consistently independent of current amplitude, indicating adequate voltage-clamp control in these experiments. When the activation curve (m_∞^3) is superimposed on the steady-state inactivation curve (Fig. 6C), there is a small amount of overlap

indicating existence of a tonically activated or 'window' current in the range of -55 to -70 mV. Since activation is modeled by m^3, voltage dependence of m is obtained as the cube root of the current activation curve, and this is also shown in Fig. 6C as the m_∞ curve.
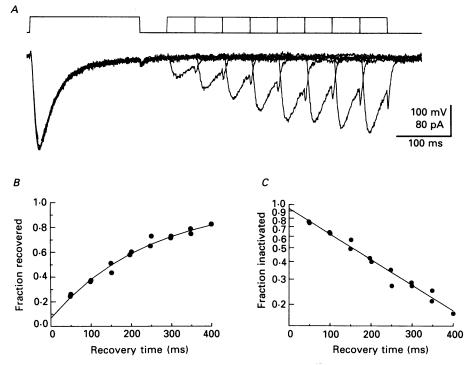

Fig. 7. Recovery from inactivation of T-current at -92 mV. A, a conditioning command step of 200 ms to -42 mV is followed by a test step at increasing latencies. These responses are the averages obtained with two identical protocols in the same cell. B, fractional recovery of T-current. C, semilogarithmic plot of recovery of inactivated current. Recovery is linear on a semilogarithmic axis indicating monoexponential decay in the time period between 50 and 400 ms. The individual data points in B and C are from two individual protocols from which the average data in A were obtained. The smooth curves are the non-linear least-squares fit function with τ of 243 ms and an initial amplitude (at 0 recovery time) of 0·07.

Recovery from inactivation of T-current in relay neurones

The frequency at which low-threshold spikes can be elicited is dependent on the process of recovery from inactivation or deinactivation (Jahnsen & Llinás, 1984a) which determines the relative refractory period. The recovery process proceeds relatively slowly at -92 mV and 23 °C, with a time constant near 230 ms (Fig. 7). Recovery after 50 ms can be fitted by a single exponential (Fig. 7B and C) that is relatively insensitive to voltage. The time constant of recovery (τ_r) was $251 \pm 10\cdot8$ ms ($N = 21$) at -92 mV compared to $225 \pm 20\cdot5$ ms ($N = 11$) at -112 mV ($P > 0\cdot05$, two-tailed t test). However, there was an early phase of more rapid recovery which accounted for approximately 20 % of the total recovery process at -92 mV. While

slow recovery (latencies greater than 50 ms) can be well fitted by an exponential process, a non-zero intercept is evident when the best-fit curves are extrapolated back to zero recovery time (Fig. 7). Although τ_r was not significantly different at potentials of -92 and -112 mV, the extrapolated zero-time fractional recoveries were ($P < 0.05$), with values of 0.19 ± 0.025 ($N = 21$) and 0.33 ± 0.058 ($N = 12$) for recovery at -92 and -112 mV, respectively. Hence recovery at early (< 50 ms) latencies was much more sensitive to recovery potential than at later times.
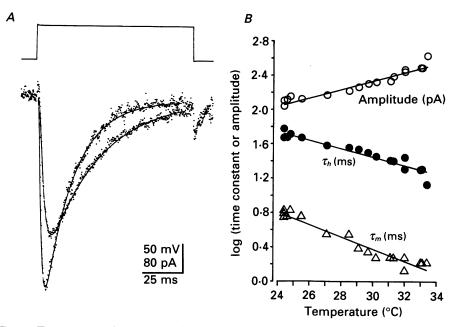

Fig. 8. Temperature dependence of activation and inactivation. A, T-currents obtained with command potential of -42 mV from a V_{hold} of -102 mV at two temperatures. Each current trace is the average of five individual traces. The smooth curves represent the best fit to m^3h kinetics. At 23·5 °C the current is smaller and slower compared to the current obtained at 28 °C. Fit parameters were $\tau_m = 2.5$ and 1·5 ms, $\tau_h = 33.1$ and 18·7 ms, and amplitude = 540 and 760 pA at 23·5 °C and 28 °C, respectively. B, in a different neurone, repeated pulses to -42 mV were applied every 30 s while the temperature was gradually increased over a period of 9 min. Curve fits were obtained for each trace, and the different fit parameters are shown in a semilogarithmic plot *vs.* bath temperature. Least-squares slopes yielded Q_{10} values of 3·1, 3·1 and 5·0 for amplitude (extrapolated zero-time amplitude), k_h ($1/\tau_h$) and k_m ($1/\tau_m$) respectively.

Temperature dependence of kinetic properties of T-current in relay neurones

In myocytes (Cavalié, McDonald, Pelzer & Trautwein, 1985), neuroblastoma (Narahashi *et al.* 1987) and invertebrate neurones (Kostyuk, Krishtal & Pidoplichko, 1981; Lux & Brown, 1984; Byerly, Chase & Stimers, 1984), Ca^{2+} currents are known to be highly temperature sensitive. In order to extrapolate the results of the present study (performed at room temperature) to the properties of T-current at body temperature, we have characterized the temperature dependence of the various kinetic parameters of the current.

In some experiments we were able to change bath temperature while maintaining stable whole-cell clamp. Under these conditions the Q_{10} for the various parameters of the Hodgkin–Huxley type model could be accurately determined within single neurones. Both activation (τ_m) and inactivation (τ_h) time constants, as well as the amplitude of the T-current were highly temperature dependent. The time course of the T-current at increasing temperatures could be well fitted with the m^3h model by changing only the time constants and amplitudes (Fig. 8A). Within the range of 24–34 °C, the temperature dependence is monophasic (Fig. 8B) and Q_{10} values were determined for each rate constant and amplitude from the slope of the semi-logarithmic function *vs.* temperature. This experiment was repeated in four cells with the following values obtained for Q_{10}: $k_m = 3\cdot55 \pm 0\cdot65$, $k_h = 2\cdot80 \pm 0\cdot27$, and amplitude $= 3\cdot30 \pm 0\cdot82$. The rate of deinactivation was also highly temperature dependent; τ_r was near 140 ms at -92 mV and 30 °C (not shown), yielding an estimated Q_{10} of 2·5 for the recovery process. The survival of isolated neurones was markedly reduced under conditions of elevated temperature and we were not able to extend the experimental conditions to include body temperatures, but the voltage-dependent parameters describing the T-current at 37 °C may be obtained by extrapolation (see below).

DISCUSSION

In this report we have examined the properties of the low-threshold, transient Ca^{2+} current in acutely dissociated mammalian central neurones. We find that several properties of this current are analogous to those of the T- or low-voltage-activated current observed in sensory neurones. Similarities include voltage dependence of activation and inactivation, permeation of Ba^{2+} comparable to Ca^{2+}, sensitivity to blockade by Ni^{2+} and relative lack of sensitivity to blockade by Cd^{2+}.

These results are in reasonable agreement with those recently obtained with switched-clamp techniques in rat and cat thalamic slices (Crunelli, Lightowler & Pollard, 1989). The only major differences are a somewhat slower inactivation rate and steeper voltage-dependent activation in slice neurones, which may be related to differences in voltage control in the more intact, less electrotonically compact cells in the slice, or pecularities of enzyme -treated acutely-isolated thalamic cells. Also, part of the discrepancy may be due to concentration of Ca^{2+} used in our experiments (3 mM), which is higher than that in the above slice study (1 mM) or in cerebrospinal fluid and the extracellular space of the brain (~ 2 mM). The increased concentration of divalent cations would increase the screening charge (Frankenhaeuser & Hodgkin, 1957; Hille, 1968), and therefore shift the voltage dependence of the gating parameters for Ca^{2+} currents. Because the $[Ca^{2+}]_o$ used in our experiments is approximately 1·5 times normal, the voltage-dependent of all kinetic properties under physiological conditions (2 mM-Ca^{2+}) would be approximately 3–4 mV less negative than reported here.

From our analysis of the kinetic parameters of the 'T-type' current, we conclude that this current underlies the low-threshold Ca^{2+} spike in thalamic relay neurones. The voltage activation range begins around -65 mV and is half-activated near -50 mV. This steep voltage dependence, along with the voltage-dependent nature of the *rate* of activation, combine to ensure the genesis of the regenerative low-

threshold spike. Small depolarizations into the threshold range of the T-current activate, with relatively slow time course, a small percentage of the total available channels. This leads to further depolarization, which activates more channels at a faster rate, and this process then continues to produce the LTS, by analogy with generation of Na^+-dependent high-threshold spikes.

Of course, other ionic conductances are activated in the same voltage range, and may reduce or enhance the LTS through hyperpolarizing or depolarizing influences. For example, a persistent Na^+ current is present in relay neurones (Jahnsen & Llinás, 1984b), which enhances the LTS by exerting a depolarizing influence. On the other hand, the Ca^{2+} that enters during the LTS will activate Ca^{2+}-dependent K^+ conductances (Deschênes *et al.* 1984; Jahnsen & Llinás, 1984b) which would tend to inhibit the LTS and/or contribute to its termination. A separate repolarizing mechanism for the LTS is probably not necessary, however, because the rate of inactivation of the T-current would be sufficiently rapid to cause termination of the LTS; since Q_{10} is greater than 2·5, τ_h would be in the range of 6–15 ms at 37 °C. This differs from the Na^+-dependent action potential in squid axon where the delayed rectifier current is required to terminate the spike (Hodgkin & Huxley, 1952), but compares with fast spike generation in myelinated axons which are lacking K^+ channels and repolarize through inactivation of Na^+ channels (Chiu, Ritchie, Rogart & Stagg, 1979).

The contribution of other types of Ca^{2+} channels to LTS generation must be minor. The maximum depolarization in the envelope of the LTS is near -35 mV (Deschênes *et al.* 1982; Jahnsen & Llinás, 1984a), and this is in the voltage range where only the low-threshold or T-current is activated. Current waveforms in this range can be well fitted with a single decay process providing evidence for a single component of current. Further support for this conclusion is obtained from the steady-state activation protocols in which the waveform does not change with holding potential. Therefore, T-current is sufficient for the activation of the LTS. The fact that it is necessary is deduced from the steady-state inactivation data. Any contribution of the high-threshold current inactivating current (N-current, Fox *et al.* 1987) would not require as much hyperpolarization to remove inactivation, since this current is half-inactivated at -70 mV. The fact that there is little or no activation of LTS at membrane potentials more positive than -65 mV argues against contributions from an N-type component. Also, the N-component does not activate until potentials are above -30 mV (Fox *et al.* 1987), outside the range for LTS activation. However, when the LTS reaches threshold for activation of Na^+-dependent action potentials, the other components of Ca^{2+} current will be activated to 'inject' additional Ca^{2+} into the cell where it can induce secondary effects such as activation of Ca^{2+}-dependent after-potentials (Deschênes *et al.* 1984; Jahnsen & Llinás, 1984b). This might be especially important for dendritic function in relay cells since the high-threshold Ca^{2+} conductance is thought to be localized there (Jahnsen & Llinás, 1984b).

The steady-state inactivation data (Fig. 6) are in general agreement with the findings of Jahnsen & Llinás (1984a). Our results would be consistent with inability to obtain an LTS at holding potentials less negative than -60 mV. However, from data such as those of Fig. 6, we assume that T-channels should become increasingly

available at potentials up to -100 mV. The fact that current-clamp experiments fail to show increasing LTS amplitude or rate of rise with hyperpolarizations beyond -75 mV might be due to the concomitant activation of anomalous rectifier current by stronger hyperpolarizations. This current would tend to shunt the T-current and reduce that amplitude of the LTS. Additionally, deinactivation of transient potassium current (A-current, Thompson, 1977; Jahnsen & Llinás, 1984b) would be enhanced by the hyperpolarization and this may also retard the development of the LTS.

Recovery from inactivation of T-current in thalamic relay neurones is not a monophasic process. While a large component of the recovery process proceeds with a τ_r of 250 ms at -92 mV, there is also an initial rapid recovery which accounts for less than half of the total. With a Q_{10} of 2·5, τ_r would be expected to be around 80 ms at 37 °C, and this is consistent with the deinactivation time course of LTS *in vitro* which is complete within 300 ms (Jahnsen & Llinás, 1984a). This is in contrast to chick sensory neurones where τ_r is approximately threefold slower (Carbone & Lux, 1987), and rat sensory neurones where recovery is biphasic with a fast component of hundreds of milliseconds and a slower component with τ_r greater than 1 s (Bossu & Feltz, 1986).

As recently emphasized by Steriade & Llinás (1988), three factors contribute to thalamocortical synchronization during quiet sleep: (1) the intrinsic properties of thalamic neurones, (2) a synaptic network that includes nucleus reticularis, and (3) the influence of brain stem reticular formation areas which project to the thalamus. The Ca^{2+}-dependent low-threshold spike is one of the intrinsic properties that is characteristic of thalamic neurones. Because T-current activation is necessary and sufficient for the generation of the LTS, modulation of this specific conductance would be expected to produce significant behavioural effects on sleep and arousal. A preliminary report suggests that endogenous neurotransmitters or neuromodulators can affect thalamic T-current, independent of their effects on membrane potential (Geijo-Barrientos & Llinás, 1988). Selective effects on T-current may also be produced by exogenous agents (Tang, Presser & Morad, 1988), including drugs used in the treatment of petit mal epilepsy (Coulter *et al.* 1989). These findings raise interesting questions about the potential role of thalamic neuronal T-current in pathophysiological processes and the effects of modulation of this important conductance by endogenous or exogenous substances.

REFERENCES

BEZANILLA, F. & ARMSTRONG, C. M. (1977). Inactivation of the sodium channel. I. Sodium current experiments. *Journal of General Physiology* **70**, 549–566.

BOSSU, J.-L. & FELTZ, A. (1986). Inactivation of the low-threshold transient calcium current in rat sensory neurones: evidence for a dual process. *Journal of Physiology* **376**, 341–357.

BYERLY, L., CHASE, P. B. & STIMERS, J. R. (1984). Calcium current activation kinetics in neurones of the snail *Lymnaea stagnalis*. *Journal of Physiology* **348**, 187–207.

CARBONE, E. & LUX, H. D. (1984). A low voltage-activated, fully inactivating Ca channel in vertebrate sensory neurones. *Nature* **310**, 501–502.

CARBONE, E. & LUX, H. D. (1987). Kinetics and selectivity of a low-voltage-activated calcium current in chick and rat sensory neurones. *Journal of Physiology* **386**, 547–570.

CAVALIÉ, A., MCDONALD, T. F., PELZER, D. & TRAUTWEIN, W. (1985). Temperature-induced transitory and steady-state changes in the calcium current of guinea-pig ventricular myocytes. *Pflügers Archiv* **405**, 294–296.

CHIU, S. Y., RITCHIE, J. M., ROGART, R. B. & STAGG, D. (1979). A quantitative description of membrane currents in rabbit myelinated nerve. *Journal of Physiology* **292**, 149–166.

COULTER, D. A., HUGUENARD, J. R. & PRINCE, D. A. (1989). Specific petit mal anticonvulsants reduce calcium currents in thalamic neurons. *Neuroscience Letters* **98**, 74–78.

CRUNELLI, V., KELLY, J. S., LERESCHE, N. & PIRCHIO, M. (1987). The ventral and dorsal lateral geniculate nucleus of the rat: intracellular recordings *in vitro*. *Journal of Physiology* **384**, 587–601.

CRUNELLI, V., LERESCHE, N. & PARNAVELAS, J. G. (1987). Membrane properties of morphologically identified X and Y cells in the lateral geniculate nucleus of the cat *in vitro*. *Journal of Physiology* **390**, 243–256.

CRUNELLI, V., LIGHTOWLER, S. & POLLARD, C. (1989). A T-type calcium current underlies the low-threshold calcium potential in cells of the cat and rat lateral geniculate nucleus. *Journal of Physiology* (in the Press).

DESCHÊNES, M., PARADIS, M., ROY, J. P. & STERIADE, M. (1984). Electrophysiology of neurons of lateral thalamic nuclei in cat: Resting properties and burst discharges. *Journal of Neurophysiology* **51**, 1196–1219.

DESCHÊNES, M., ROY, J. P. & STERIADE, M. (1982). Thalamic bursting mechanism: an inward slow current revealed by membrane hyperpolarization. *Brain Research* **239**, 289–293.

FOX, A. P., NOWYCKY, M. C. & TSIEN, R. W. (1987). Kinetic and pharmacological properties distinguishing three types of calcium currents in chick sensory neurones. *Journal of Physiology* **394**, 149–172.

FRANKENHAEUSER, B. & HODGKIN, A. L. (1957). The action of calcium on the electrical properties of squid axons. *Journal of Physiology* **137**, 218–244.

FRIEDMAN, A. & GUTNICK, M. J. (1987). Low-threshold calcium electrogenesis in neocortical neurons. *Neuroscience Letters* **81**, 117–122.

GEIJO-BARRIENTOS, E. & LLINÁS, R. (1988). Dopamine and haloperidol modify low threshold calcium spike and transient calcium current in guinea pig thalamic neurons *in vitro*. *Society for Neuroscience Abstracts* **14**, 932.

GOLDMAN, D. E. (1943). Potential, impedance and rectification in membranes. *Journal of General Physiology* **27**, 37–60.

GREENE, R. W., HAAS, H. L. & MCCARLEY, R. W. (1986). A low threshold calcium spike mediates firing pattern alterations in pontine reticular neurones. *Science* **234**, 738–740.

HAGIWARA, S. & OHMORI, H. (1982). Studies of calcium channels in rat clonal pituitary cells with patch electrode voltage-clamp. *Journal of Physiology* **331**, 231–252.

HAMILL, O. P., MARTY, A., NEHER, E., SAKMANN, B. & SIGWORTH, F. J. (1981). Improved patch-clamp techniques for high-resolution current recording from cells and cell-free membrane patches. *Pflügers Archiv* **391**, 85–100.

HARRIS, R. M. & HENDRICKSON, A. E. (1987). Local circuit neurons in the rat ventrobasal thalamus – a GABA immunocytochemical study. *Neuroscience* **21**, 229–236.

HILLE, B. (1968). Charges and potentials at the nerve surface. *Journal of General Physiology* **51**, 221–236.

HODGKIN, A. L. & HUXLEY, A. F. (1952). A quantitative description of membrane current and its application to conduction and excitation in nerve. *Journal of Physiology* **117**, 500–544.

HODGKIN, A. L. & KATZ, B. (1949). The effect of sodium ions on the electrical activity of the giant axon of the squid. *Journal of Physiology* **108**, 37–77.

HUGUENARD, J. R. & ALGER, B. E. (1986). Whole-cell voltage-clamp study of the fading of GABA-activated currents in acutely dissociated hippocampal neurons. *Journal of Neurophysiology* **56**, 1–18.

JAHNSEN, H. & LLINÁS, R. (1984a). Electrophysiological properties of guinea-pig thalamic neurones: an *in vitro* study. *Journal of Physiology* **349**, 205–226.

JAHNSEN, H. & LLINÁS, R. (1984*b*). Ionic basis for the electroresponsiveness and oscillatory properties of guinea-pig thalamic neurones *in vitro*. *Journal of Physiology* **349**, 227–247.

JONES, E. G. (1985). *The Thalamus*. New York: Plenum Press.

KAY, A. R. & WONG, R. K. S. (1986). Isolation of neurons suitable for patch-clamping from adult mammalian central nervous systems. *Journal of Neuroscience Methods* **16**, 227–238.

KAY, A. R. & WONG, R. K. S. (1987). Calcium current activation kinetics in isolated pyramidal neurons of the CA1 region of the mature guinea-pig hippocampus. *Journal of Physiology* **392**, 603–616.

KOSTYUK, P. G., KRISHTAL, O. A. & PIDOPLICHKO, V. I. (1981). Calcium inward current and related charge movements in the membrane of snail neurones. *Journal of Physiology* **310**, 403–421.

LLINÁS, R. & YAROM, Y. (1981). Properties and distribution of ionic conductances generating electroresponsiveness of mammalian inferior olivary neurones *in vitro*. *Journal of Physiology* **315**, 569–584.

LUX, H. D. & BROWN, A. M. (1984). Patch and whole cell calcium currents recorded simultaneously in snail neurons. *Journal of General Physiology* **83**, 727–750.

NARAHASHI, T., TSUNOO, A. & YOSHII, M. (1987). Characterization of two types of calcium channels in mouse neuroblastoma cells. *Journal of Physiology* **383**, 231–249.

NOWYCKY, M. C., FOX, A. P. & TSIEN, R. W. (1985). Three types of neuronal calcium channel with different calcium agonist sensitivity. *Nature* **316**, 440–443.

NUMANN, R. E. & WONG, R. K. S. (1984). Voltage-clamp study on GABA response desensitization in single pyramidal cells dissociated from the hippocampus of adult guinea pigs. *Neuroscience Letters* **47**, 289–294.

SCHREINER, W., KRAMER, M., KRISCHER, S. & LANGSAM, Y. (1985). Nonlinear least-squares fitting. *PC Technical Journal* **3**, 170–181.

STERIADE, M. & LLINÁS, R. R. (1988). The functional states of the thalamus and the associated neuronal interplay. *Physiological Reviews* **68**, 649–742.

TANG, C.-M., PRESSER, F. & MORAD, M. (1988). Amiloride selectively blocks the low threshold (T) calcium channel. *Science* **240**, 213–215.

THOMPSON, S. H. (1977). Three pharmacologically distinct potassium channels in molluscan neurones. *Journal of Physiology* **265**, 465–488.

WILCOX, K. S., GUTNICK, M. J. & CHRISTOPH, G. R. (1988). Electrophysiological properties of neurons in the lateral habenula nucleus: an *in vitro* study. *Journal of Neurophysiology* **59**, 212–225.